Solid State Communications,Vol. 19, pp. 845–851, 1976. Pergamon Press. Printed in Great Britain

MAGNETIC STRUCTURE OF YMn_{12}

J. Deportes and D. Givord

Laboratoire de Magnétisme, C.N.R.S., 166-X, 38042 Grenoble Cedex, France

(*Received* 12 *April* 1976 *by E.F. Bertaut*)

YMn_{12} crystallizes in the I_4/mmm tetragonal body-centred sturcture. Neutron diffraction experiments give evidence for an antiferromagnetic structure ($T_N = 120$ K) in the tetragonal cell. The magnetic structure has been determined with the help of group theory. The mean Mn magnetic moment is $0.4\mu_B$. In spite of the non-colinear arrangement of magnetic moments strong negative anisotropic interactions are evidenced. As it is observed in pure Mn and in rare earth–Fe compounds, these interactions are strongly distance dependent.

1. INTRODUCTION

THE PHASE DIAGRAMS of rare earth (R)–transitions metal rich (M) compounds give evidence for numerous well-defined compounds the stoichiometries which are between RM_2 and RM_{12}.[1] Their structures are all derived from the fundamental basis of $CaCu_5$-type. The RM_5 phase stability and the number of compounds in each series depend on the alloyed transition metal. Many compounds are obtained with Ni and Co. The Fe compounds are less numerous; the RM_2 and RMn_{12} compounds are the only manganese compounds related with the $CaCu_5$-type structure. Few studies concern these last compounds because of the difficulties of elaboration. We have obtained pure RM_{12} compounds, with Y and the heavy rare earth metals, using a levitation furnace. The YMn_{12} behaviour is characteristic of an antiferromagnetic compound; the Néel temperature is $T_N =$ 120 K.[2] We present, in this paper, the determination by neutron diffraction of the arrangement of the magnetic moments below the ordering temperature.

2. PREPARATION

The RMn_{12} compounds crystallize in the tetragonal $ThMn_{12}$-type structure (I_4/mmm). They are obtained by peritectic reaction; due to the high value of the vapour pressure of manganese, the preparation is made difficult.[3] Samples were prepared by melting the constituents (purity 99.9%) in a levitation furnace and subsequently quenching them from the melt in a copper ingot mold. To compensate for the loose due to Mn evaporation during melting, the starting composition was $RMn_{12.5}$. The alloy thus obtained always contained as impurities a large amount of the two neighbouring phases, Y_6Mn_{23} and pure Mn. After annealing for 8 days at 1000°C in sealed quartz tube, these impurities were no more observed by X-ray diffraction.

Table 1. Position parameters of Y *and* Mn *atoms in the crystallographic body-centered tetragonal cell* (*space group* I_4/mmm): a = *8.59* Å; c = *4.79* Å

Y 2*a*				
1: 0 0 0	2: $\frac{1}{2}\ \frac{1}{2}\ \frac{1}{2}$			
Mn 8*i*				
1: $x, 0, 0$	2: $\bar{x}, 0, 0$	3: $0, x, 0$	4: $0, \bar{x}, 0$	$x = 0.36$
5: $\frac{1}{2}+x, \frac{1}{2}, \frac{1}{2}$	6: $\frac{1}{2}-x, \frac{1}{2}, \frac{1}{2}$	7: $\frac{1}{2}, \frac{1}{2}+x, \frac{1}{2}$	8: $\frac{1}{2}, \frac{1}{2}-x, \frac{1}{2}$	
8*j*				
1: $x, \frac{1}{2}, 0$	2: $\bar{x}, \frac{1}{2}, 0$	3: $\frac{1}{2}, x, 0$	4: $\frac{1}{2}, \bar{x}, 0$	$x = 0.277$
5: $\frac{1}{2}+x, 0, \frac{1}{2}$	6: $\frac{1}{2}-\bar{x}, 0, \frac{1}{2}$	7: $0, \frac{1}{2}+x, 0$	8: $0, \frac{1}{2}-x, 0$	
8*f*				
1: $\frac{1}{4}, \frac{1}{4}, \frac{1}{4}$	2: $\frac{3}{4}, \frac{3}{4}, \frac{1}{4}$	3: $\frac{1}{4}, \frac{3}{4}, \frac{1}{4}$	4: $\frac{3}{4}, \frac{1}{4}, \frac{1}{4}$	
5: $\frac{3}{4}, \frac{3}{4}, \frac{3}{4}$	6: $\frac{1}{4}, \frac{1}{4}, \frac{3}{4}$	7: $\frac{3}{4}, \frac{1}{4}, \frac{3}{4}$	8: $\frac{1}{4}, \frac{3}{4}, \frac{3}{4}$	

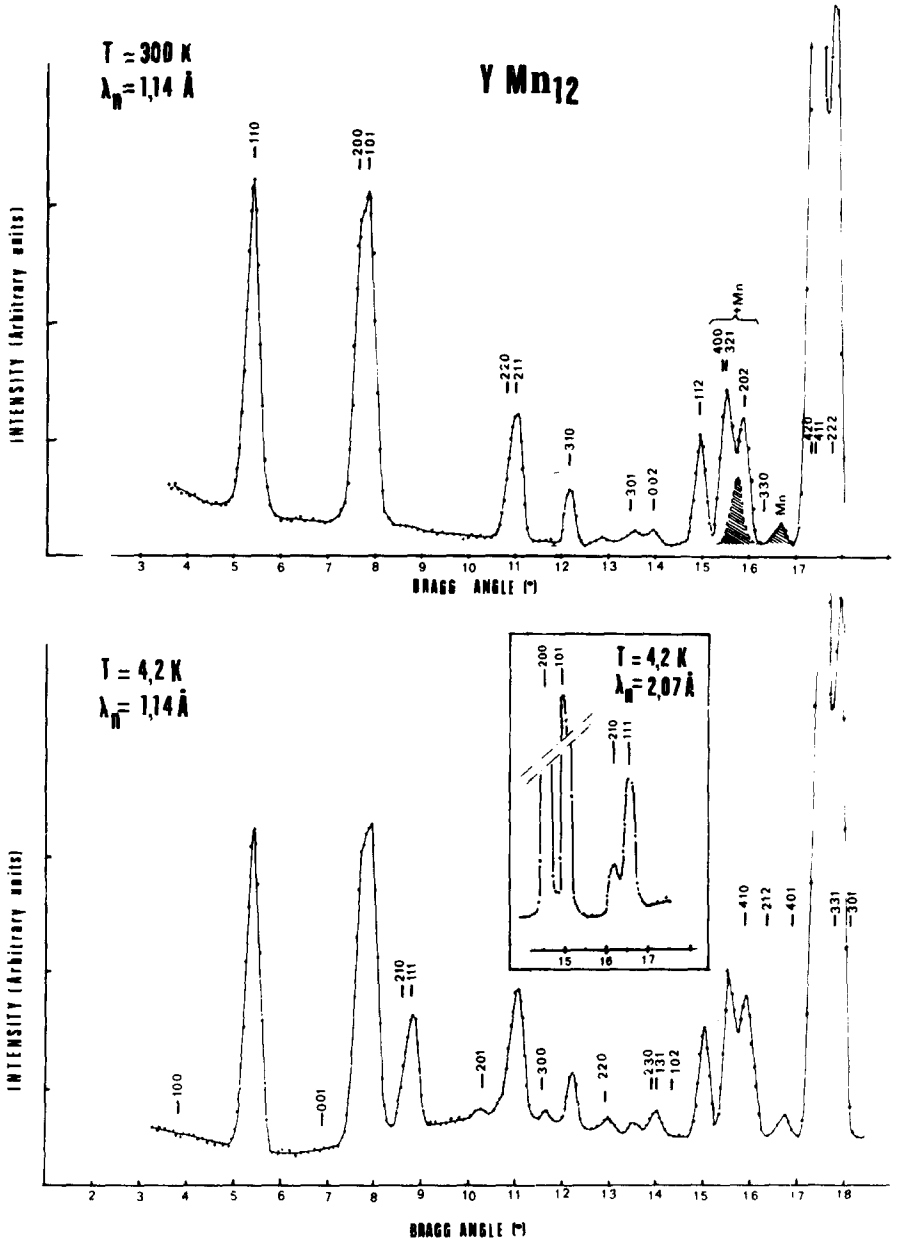

Fig. 1. Neutron diffraction pattern of YMn_{12}.

A Debye–Scherrer pattern of YMn_{12} can be indexed in a body-centered cell, with parameters $a = 8.59$ Å and $c = 4.79$ Å. This crystallographic cell is double, it contains 2 yttrium atoms in 2*a* positions and 24 manganese atoms lying in 3 different sites (8*i*, 8*j* and 8*f*) (Table 1). The magnetic arrangement on each of these sites has been determined by neutron diffraction experiments performed at the "Centre d'Etudes Nucléaires de Grenoble". Neutron diffraction patterns have been obtained with neutrons of wavelength $\lambda_n = 1.14$ and 2.07 Å at temperatures ranging from 4.2 to 300 K.

3. RESULTS

Figure 1 shows the neutron diffraction patterns obtained at 300 and 4.2 K with YMn_{12}. At 300 K, the compound is paramagnetic. In fact, the observed diffraction lines are interpreted by the nuclear coherent scattering alone. They can be indexed in the tetragonal crystallographic cell. The conditions of possible reflections ($h + k + l = 2n$) characteristic of a body-centered structure are obeyed. Two weak additional lines are observed, they correspond to the most intense

Table 2. Calculated and observed intensities at 300 and 4.2 K

	$T = 300$ K				$T = 4.2$ K		
$h\,k\,l$	θ	I_{obs}	I_{cal} Nucl.	$h\,k\,l$	θ	I_{obs}	I_{cal} Mag.
1 1 0	5.4	35.5	35.0	1 0 0	3.81	n.o.	0.1
2 0 0	7.64	100	41	0 0 1	6.88	n.o.	–
1 0 1	7.87		61	2 1 0	8.55	4	4
2 2 0	10.84	55.2	15	1 1 1	8.72	22	22.4
2 1 1	11		44	2 0 1	10.3	3	1.3
3 1 0	12.14	30	24	3 0 0	11.5	1	0.5
3 0 1	13.45		1	2 2 1	12.9	2.3	1.9
0 0 2	13.85	19.2	3.3	2 3 0	13.87	4.8	1.4
1 1 2	14.9		65	1 3 1	14		3
4 0 0	15.42	69	61	1 0 2	14.35	n.o.	0.8
3 2 1	15.54	118	33	3 0 2	15.15		0.8
2 0 2	15.90		51	1 4 0	15.9	8	7.4
3 3 0	16.4	0	1	2 1 2	16.4		0.9
4 2 0	17.30		315	4 0 1	16.9	n.o.	0.01
4 1 1	17.41	1232.5	433	3 3 1	17.8	6	5.6
2 2 2	17.73		468				

reflections ((330)–(411), (332)) of the α-Mn phase. The observed intensities are listed in Table 2; they are compared with those calculated using the position parameters reported in Table 1 and the neutron Fermi length $b_Y = 0.80 \times 10^{-12}$ cm $b_{Mn} = -0.36 \times 10^{-12}$ cm. The agreement factor $R = \Sigma(I_{obs} - I_{calc})/\Sigma I_{obs}$ is 3.5%.

At 4.2 K, the intensities of the lines of indices $(h + k + l = 2n)$ are not modified (Table 2). New lines appear; they can also be indexed in the crystallographic cell, but they obey the condition $h + k + l = 2n + 1$. The (100) and (001) reflections are not observed, the contributions to the (300), (201) reflections are weak. Of these new lines, the most intense contribution is observed at a Bragg angle $\theta = 8.7°$. It corresponds to the (210) and (111) reflections which are not resolved with neutron of wavelength $\lambda_n = 1.14$ Å. The intensity of each of these two reflections has been measured from a pattern obtained with neutrons of wavelength $\lambda_n = 2.07$ Å (Fig. 1, insert).

These lines observed at 4.2 K are characteristic of an antiferromagnetic ordering inside the tetragonal crystallographic cell. The propagation vector K of the magnetic structure is $K = [001]$, the structure being anticentered: the magnetic moments deduced by the translation $I(\frac{1}{2}\,\frac{1}{2}\,\frac{1}{2})$ are antiparallel. The neutron diffraction patterns obtained at temperature lower than the Néél temperature (120 K) present all the same additional lines associated with the magnetic order.

4. DETERMINATION OF THE MAGNETIC STRUCTURE

The large number (24) of magnetic atoms in the YMn_{12} cell makes it difficult to determine *a priori* a model of magnetic structure in agreement with the observed neutron diffraction patterns. Therefore, we have considered all the arrangements of the magnetic moments allowed by group theory. The different possible models were determined with the help of the macroscopic theory developed by Bertaut.[4] In each case, the calculated intensities of the diffraction lines were compared to the experimental results. The propagation vector K of the magnetic structure being a vector of the reciprocal lattice, we have determined the linear combinations of magnetic moments which are the base vectors associated with the irreducible representations of the I_4/mmm space group. This group is the semi-direct product of the point group P_4/mmm by the translation group T, the elements of which are the lattice translations and the translation $I(\frac{1}{2}\,\frac{1}{2}\,\frac{1}{2})$. The irreducible representations of the group P_4/mmm are listed in Table 3. Often, when a magnetic structure is centered or anticentered, only those magnetic moments belonging to the primitive group may be considered. In YMn_{12} this simplification is not possible; in fact, the translation $I(\frac{1}{2}\,\frac{1}{2}\,\frac{1}{2})$ is equivalent, for the $8f$ site, to the inversion operation $\bar{1}$; therefore the multiplicity of the

Table 3. Irreducible representations of the group P4/mmm. E, 4^2, 4, . . . *are the ordinary symbols of the different symmetry operators. In the representations* Γ_i ($i = 1, 2, 3, 4, 5$) *the* D *matrix of the inverse operator 1 is* $\mathbb{1}$: $D(\bar{1}) = \mathbb{1}$. *In the representations* Γ'_1 ($i = 1, 2, 3, 4, 5$), $D(1) = -\mathbb{1}$

Γ_1	E	4^2	4	4^3	2_x	2_y	2_{xy}	2_y	$\bar{1}$	m_z	$\bar{4}$	$4m_z$	m_x	m_y	m_{xy}	m_{yz}
Γ_1	1	1	1	1	1	1	1	1	1	1	1	1	1	1	1	1
Γ_2	1	1	1	1	−1	−1	−1	−1	1	1	1	1	−1	−1	−1	−1
Γ_3	1	1	−1	−1	1	1	−1	−1	1	1	−1	−1	1	1	−1	−1
Γ_4	1	1	−1	−1	−1	−1	1	1	1	1	−1	−1	−1	−1	1	1
Γ_5	$\begin{pmatrix} 1 & \cdot \\ \cdot & 1 \end{pmatrix}$	$\begin{pmatrix} -1 & \cdot \\ \cdot & -1 \end{pmatrix}$	$\begin{pmatrix} -1 & \cdot \\ \cdot & 1 \end{pmatrix}$	$\begin{pmatrix} \cdot & 1 \\ -1 & \cdot \end{pmatrix}$	$\begin{pmatrix} 1 & \cdot \\ \cdot & -1 \end{pmatrix}$	$\begin{pmatrix} -1 & \cdot \\ \cdot & 1 \end{pmatrix}$	$\begin{pmatrix} \cdot & -1 \\ -1 & \cdot \end{pmatrix}$	$\begin{pmatrix} \cdot & 1 \\ 1 & \cdot \end{pmatrix}$	$\begin{pmatrix} 1 & \cdot \\ \cdot & 1 \end{pmatrix}$	$\begin{pmatrix} -1 & \cdot \\ \cdot & -1 \end{pmatrix}$	$\begin{pmatrix} \cdot & -1 \\ 1 & \cdot \end{pmatrix}$	$\begin{pmatrix} \cdot & 1 \\ -1 & \cdot \end{pmatrix}$	$\begin{pmatrix} 1 & \cdot \\ \cdot & -1 \end{pmatrix}$	$\begin{pmatrix} -1 & \cdot \\ \cdot & 1 \end{pmatrix}$	$\begin{pmatrix} \cdot & -1 \\ -1 & \cdot \end{pmatrix}$	$\begin{pmatrix} \cdot & 1 \\ 1 & \cdot \end{pmatrix}$
Γ'_1	1	1	1	1	1	1	1	1	−1	−1	−1	−1	−1	−1	−1	−1
Γ'_2	1	1	1	1	1	−1	−1	−1	−1	−1	−1	−1	−1	−1	1	−1
Γ'_3	1	1	−1	−1	1	1	−1	−1	−1	−1	1	1	−1	−1	1	1
Γ'_4	1	1	−1	−1	−1	−1	1	1	−1	−1	1	1	1	1	−1	−1
Γ'_5	$\begin{pmatrix} 1 & \cdot \\ \cdot & 1 \end{pmatrix}$	$\begin{pmatrix} -1 & \cdot \\ \cdot & -1 \end{pmatrix}$	$\begin{pmatrix} \cdot & -1 \\ 1 & \cdot \end{pmatrix}$	$\begin{pmatrix} \cdot & 1 \\ -1 & \cdot \end{pmatrix}$	$\begin{pmatrix} 1 & \cdot \\ \cdot & -1 \end{pmatrix}$	$\begin{pmatrix} -1 & \cdot \\ \cdot & 1 \end{pmatrix}$	$\begin{pmatrix} \cdot & -1 \\ -1 & \cdot \end{pmatrix}$	$\begin{pmatrix} \cdot & 1 \\ 1 & \cdot \end{pmatrix}$	$\begin{pmatrix} -1 & \cdot \\ \cdot & -1 \end{pmatrix}$	$\begin{pmatrix} 1 & \cdot \\ \cdot & 1 \end{pmatrix}$	$\begin{pmatrix} \cdot & 1 \\ -1 & \cdot \end{pmatrix}$	$\begin{pmatrix} \cdot & -1 \\ 1 & \cdot \end{pmatrix}$	$\begin{pmatrix} -1 & \cdot \\ \cdot & 1 \end{pmatrix}$	$\begin{pmatrix} 1 & \cdot \\ \cdot & -1 \end{pmatrix}$	$\begin{pmatrix} \cdot & 1 \\ 1 & \cdot \end{pmatrix}$	$\begin{pmatrix} \cdot & -1 \\ -1 & \cdot \end{pmatrix}$

Table 4. Base vectors of the irreducible representation for the 8i and 8j sites. F, G, C, A *symbols have their usual meaning for signs alternance; their indices 1 or 5 are related to the arrangement of the magnetic moment of atoms 1, 2, 3, 4 or 5, 6, 7, 8 (according to Table 1);* x *and* y *indices refer to [100] and [010] crystallographic directions. As examples:* G_{1xy} *means:* $S_{1x} - S_{2y} + S_{3x} - S_{4y}$; F_{5z} *means:* $S_{5z} + S_{6z} + S_{7z} + S_{8z}$

Γ_1	0	0	0
Γ_2	0	0	$F_{1z} - F_{5z}$
Γ_3	0	0	0
Γ_4	0	0	$C_{1z} - C_{5z}$
Γ_5	$(S_{1x} + S_{2x} - S_{5x} - S_{6x}) \pm (S_{3x} + S_{4x} - S_{7x} - S_{8x})$ $(S_{1y} + S_{2y} - S_{5y} - S_{6y}) \pm (S_{3y} + S_{4y} - S_{7y} - S_{8y})$		0
Γ'_1	$G_{1xy} - G_{5xy}$	0	0
Γ'_2	0	$A_{1yx} - A_{5yx}$	0
Γ'_3	$A_{1xy} - A_{5xy}$	0	0
Γ'_4	0	$G_{1xy} - G_{5xy}$	0
Γ'_5	0	0	$-S_{3z} + S_{4z} + S_{7z} - S_{8z}$
	0	0	$S_{1z} - S_{2z} - S_{5z} + S_{6z}$

Table 5. Base vectors of the irreducible representations for the 8f site

Γ_1	0	0	0
Γ_2	0	0	0
Γ_3	0	0	0
Γ_4	0	0	0
Γ_5	0	0	0
Γ'_1	$G_{1x} - G_{5x} + A_{1y} - A_{5y}$		$F_{1z} - F_{5z}$
Γ'_2	$A_{1x} - A_{5x} - G_{1y} + G_{5y}$		0
Γ'_3	$G_{1x} - G_{5x} - A_{1y} + A_{5y}$		0
Γ'_4	$A_{1x} - A_{5x} + G_{1y} - G_{5y}$		$C_{1z} - C_{5z}$
Γ'_5	$(C_{1x} - C_{5x}) \pm (F_{1y} - F_{5y})$		$A_{1z} - A_{5z}$
	$(F_{1x} - F_{5x}) \pm (C_{1y} - C_{5y})$		$-G_{1z} + G_{5z}$

8*f* site is not reduced when suppressing the operation *I*. Consequently, we have considered the representations of the I_4/mmm group for $k = [001]$, deduced from those of the P_4/mmm group, taking the *D*-matrix which represents the translation *I* as $-\mathbb{1}$: $D(I) = -\mathbb{1}$. The base vectors of the irreducible representations were obtained by the technique of the projection operator. They are listed in Table 4 for the 8*i* and 8*j* sites, in Table 5 for the 8*f* site.

In the representation $\Gamma_i[D(\bar{1}) = \mathbb{1}]$, no antiferromagnetic arrangement is allowed on the 8*f* site. However, assuming that the 8*f* atoms are not magnetic, we have searched for an antiferromagnetic structure, on 8*i* and 8*j* sites, in agreement with the observed intensities. The arrangements F_z and G_z associated with the one-dimensional Γ_2 and Γ_4 representations would lead to a large contribution on the (100) line which is not observed. In the two-dimensional Γ_5 representation, the magnetic moments are perpendicular to the *c*-axis. All the magnetic structures are such that either the (001) reflection is calculated to be intense, or the (111) one calculated to be nul. No magnetic structure associated with the Γ_i representations can therefore give account for the experimental neutron diffraction results.

In the Γ'_i representations $[D(\bar{1}) = -\mathbb{1}]$, magnetic arrangements are allowed on each of the three crystallographic sites of manganese. Collinear structures are associated with the Γ'_5 two-demensional representations, the magnetic moments being parallel to the *c*-axis. The calculated intensities for each possible arrangement are not in agreement with the experimental results: either the (100) reflection is calculated too large, or the (210) reflection is calculated more intense than the (111). The other arrangements associated with the Γ'_1 representations are all non collinear. In the Γ'_5 representation, non-collinear structures are also allowed; arrangements described by

$$(C_{1x} - C_{5x}) \pm (F_{1y} - F_{5y})$$
$$(F_{1x} - F_5) \pm (C_{1y} - C_{5y})$$

are possible on the 8*f* site but the (001) reflection which is not observed should be intense. The Γ'_1 and Γ'_3 representations may be rejected because the (201) and (300) reflections are then not allowed although they are experimentally observed. Only one-dimensional Γ'_2 and Γ'_4 representations are left to be considered. Assuming the same value for the Mn moment on each crystallographic site, no solution is in good agreement with the experimental results. In a structure belonging to the Γ'_2 representation, a good reliability factor is obtained, attributing a magnetic moment 3 times smaller on the 8*f* site than on the 8*i* and 8*j* sites. The structure is then described by the combination of the arrangements on the three sites:

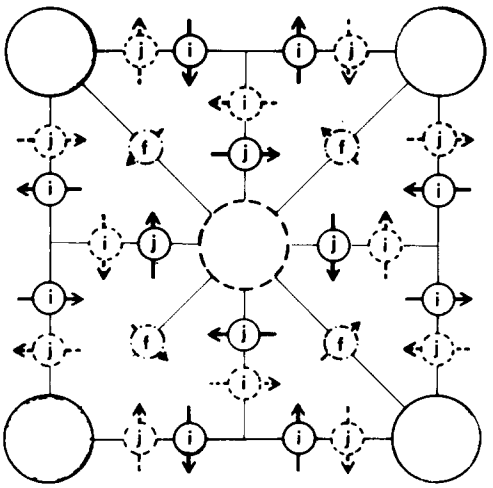

Fig. 2. Magnetic structure of YMn_{12}: Y atoms are represented by large circles, Mn atoms by small circles; atoms drawn with full lines lie in the plane $z = 0$, those drawn with dashed lines lie in the plane $z = \frac{1}{2}$. The Mn atoms on the f site (dashed–dotted lines) lie in the planes $z = \frac{1}{4}$ and $z = \frac{3}{4}$.

5. DISCUSSION AND CONCLUSION

In the YMn_{12} crystallographic structure, each manganese atom lies in a mirror plane which contains the c-axis; in the magnetic structure, each magnetic moment is perpendicular to this mirror plane. The Shubnikov group of the magnetic structure is $I_p4/m'mm$, the direction of each magnetic moment is known without ambiguity. The mirror planes containing the atoms being elements of the magnetic group, a given magnetic moment must transform into itself through the associated mirror plane. That is possible only if each magnetic moment is perpendicular to this mirror plane.

Although the YMn_{12} magnetic structure is not collinear, the arrangements of magnetic moments between first neighbouring atoms are nearly collinear. In Fig. 3, we have represented the arrangement of the magnetic moments around a Mn atom of each of the three crystallographic sites. On each site, the magnetic moment direction is determined by the molecular field deduced from isotropic exchange interactions with all the first neighbouring atoms. The inequalities between

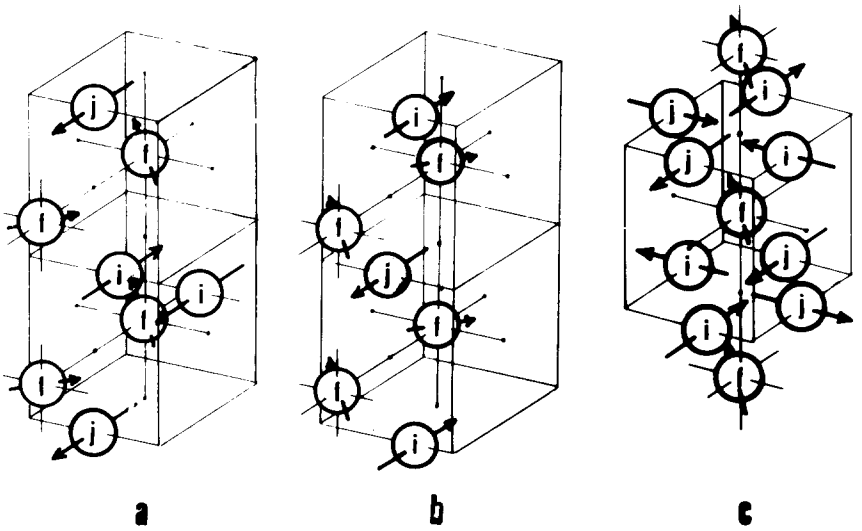

Fig. 3. Arrangements of magnetic moments around Mn atoms of each of the three crystallographic sites. Taking into account isotropic interactions between first neighbouring atoms alone, defined by $J_{ii}, J_{ij}, J_{if}, J_{jf}$, the following inequalities are deduced: (a) $J_{ii} + 2J_{ij} + (2\sqrt{2}/3)J_{if} < 0$; (b) $2J_{ij} - (2\sqrt{2}/3)J_{jf} < 0$; (c) $2\sqrt{2}J_{fi} - 2\sqrt{2}J_{fj} + \frac{2}{3}J_{ff} < 0$. The relations (a) and (b) indicate that J_{ii} and J_{ij} are strongly negative. According to (c) the molecular field on the f site may result from competitive interactions.

$$(A_{1yx} - A_{5yx})_i - (A_{1yx} - A_{5yx})_j + (A_{1x} - A_{5x} - G_{1y} + G_{5y})_f.$$

In Table 2, the calculated magnetic intensities are compared to the observed ones. The $3d$-type Mn form factor, as calculated by Freeman and Watson[5] has been used. The Mn magnetic moment is $0.42 \pm 0.04\mu_B$ on $8i$ and $8j$ sites, and $0.14 \pm 0.04\mu_B$ on the $8f$ site. The reliability factor R is 8%. The non-collinear magnetic structure is schematized on Fig. 2.

exchange interactions, deduced from the stability conditions, are indicated in the caption of Fig. 3.

YMn_{12} does not exhibit a spontaneous magnetization; its Néel temperature is high (120 K), the arrangements shown in Fig. 3 give evidence for many antiparallel couplings. These properties must be explained by large negative exchange interactions associated with the short interatomic distances (2.4–2.5 Å). The magnetic structure is built from arrangements identical to those of Fig. 3. The perpendicular couplings which

appear between atoms belonging to two neighbouring arrangements are associated with interatomic distances close to 2.7 Å. Under the hypothesis of isotropic magnetic exchange, the interactions associated with these distances must be weak. All these properties are due to the strong dependence of magnetic interactions with distance:[6] strongly negative for short interatomic distances, they vanish at about 2.7 Å. These results are in excellent agreement with the dependence of the exchange interactions on the interatomic distances found in α-Mn.[7]

In conclusion, in R–Co and R–Ni compounds, where the Curie temperature is an almost linear function of the square of the magnetic moment, the magnetic interactions depend essentially on the modification of the $3d$-band associated with the transfer of rare earth conduction electrons.[8] In R–Mn compounds, as in R–Fe ones,[9] the magnetic interactions vary strongly with distances, The magnetic properties are mainly determined by interatomic distances and the number of nearest neighbours. However, in Mn alloys, the negative interactions play a major role.

Acknowledgements – Dr. R. Lemaire has proposed this study and it is a pleasure to thank him for his suggestions and his constant interest in this work. We are also very grateful to Dr. P. Wolfers for many helpful discussions concerning mainly group theory.

1. WALLACE W.E., *Rare Earth Intermetallics.* Academic Press, London (1971).
2. DEPORTES J., GIVORD D., LEMAIRE R., NAGAI H. & YANG Y.T. (to be published).
3. KIRCHMAYR H.R., *IEEE Trans. Magn.* **MAG2–3**, 493 (1966).
4. BERTAUT E.F., *Acta Crystallogr.* **A24**, 217 (1968).
5. FREEMAN A.J. & WATSON R.E., *Acta Crystallogr.* **14**, 231 (1961).
6. NEEL L., *Ann. Phys.* **5**, 232 (1936).
7. YAMADA T., KUNITOMI N., NAKAI Y., COX D.E. & SHIRANE D., *J. Phys. Soc. Japan* **28–3**, 615 (1970).
8. BARBARA B., GIGNOUX D., GIVORD D., GIVORD F. & LEMAIRE R., *Int. J. Magn.* **4**, 77 (1973).
9. GIVORD D. & LEMAIRE R., *IEEE Trans. Magn.* **MAG10–2**, 109 (1974).